Simulating Aggregation and Reaction: New Hounslow DPB and Four-Parameter Summary

E. J. W. Wynn
The Centre for Formulation Engineering, University of Birmingham, Edgbaston, Birmingham B15 2TT, U.K.

A new formulation is developed of the popular Discretized Population Balance due to Hounslow and co-workers. This new formulation is simpler and permits some variations in the method; three variations are put forward and tested. It also allows more flexibility in the choice of discretization, so that detail can be added at small sizes. The method is applied to the case of free-molecular aggregation of SiO_2 molecules in flames. The SiO_2 is in equilibrium with SiO, which is assumed not to participate in aggregation; SiO_2 molecules are, therefore, continuously created during aggregation. This source term complicates the resulting particle-size distributions compared to the self-preserving size distribution. Four parameters are used to summarize the PSDs, and their rates of change are found by approximations. This summarized model, a quasi-self-preserving size distribution, matches the detailed simulations very well. The cause of the stiffness of the differential equations is shown to be collisions between small and large particles. © 2004 American Institute of Chemical Engineers *AIChE J,* 50: 578–588, 2004
Keywords: aggregation, self-preserving particle size distribution (SPSD), population balance equations, free molecular regime

Introduction

The numerical solution of population balance equations (PBEs) is the most popular approach for simulating particle-size distributions (PSDs) in particulate processes such as aggregation, crystal growth, and breakage (Randolph and Larson, 1988). Discretized population balances (DPBs) are often the most straightforward numerical method, although there are alternatives, such as reconstruction from moments or assumed-shape distributions (Xiong and Pratsinis, 1991), Monte-Carlo methods (Wu and Friedlander, 1993), finite elements (Nicmanis and Hounslow, 1998), and moving boundaries (Kumar and Ramkrishna, 1997). In particular, DPBs represent the PSD by discretization—that is, by a vector of quantities corresponding to fixed size intervals—which is useful if particles are exchanged across other coordinates (internal or external), because the representations of the PSDs are compatible with each other.

The Hounslow DPB is a very popular method in many applications involving aggregation (for example, Tsantilis and Pratsinis, 2000; Biggs and Lant, 2002). It has been adapted from its original format (Hounslow et al., 1988) to permit adjustable interval spacings (Litster et al., 1995). A minor correction should also be noted (Wynn, 1995). It has the major advantage of guaranteeing correct prediction of the total number and mass of particles. In the current work, a new, simpler formulation is given for the Hounslow DPB for aggregation. Using this, variations are suggested and compared. One variation is applied to the aggregation of very small particles in flames. The resulting PSDs can be summarized using just four parameters, whose rates of change can be predicted by approximations. Thus, only four differential equations are needed to simulate aggregation with a continuous source of primary particles. It is shown that the stiffness in the differential equations for free-molecular aggregation derives from collisions between small and large particles, particularly the effect of these collisions on large particles when most particles are small, and vice versa.

New Formulation of the Hounslow DPB

The adjustable Hounslow DPB (Litster et al., 1995) sets out to find all the aggregation events that can change the number of particles in the i^{th} size interval. (This interval is defined as particle volumes v in the range $v_i \leq v < v_{i+1}$. The intervals are assumed to be in geometric progression, with constant $r \equiv (v_{i+1}/v_i) = 2^{1/q}$, where q is an integer.) The aggregation

events are divided into five types, and each of the five types involves a range of other intervals. The "natural" rates of these various events are calculated, and then some rates are adjusted to guarantee correct prediction of total number and mass of particles. The resulting formulas are somewhat complicated, although quick to calculate.

An alternative approach, developed here, is to consider the result of aggregation events between the i^{th} and j^{th} size intervals, rather than starting at the result and deducing ranges of i and j. This approach is simplified by an important observation for a discretization with sizes in geometric progression: the convolution of two size intervals (say, i and j) will always be contained within two intervals (say, $k-1$ and k). In other words, when particles from interval i aggregate with those from j, the resulting aggregates will fall into the two intervals. For clarity, we will insist that $i \le j$, and it is clear that $k > j$ (although $k-1$ will equal j for small i). The observation can easily be justified: if the smallest aggregate falls within the $(k-1)^{\text{th}}$ interval, that is

$$v_{k-1} \le (v_i + v_j) < v_k \tag{1}$$

then by multiplying all quantities by r, it can be seen that the largest aggregate, with volume $(v_{i+1} + v_{j+1})$, will fall within the next highest interval. For $r = 2^{1/q}$, then $i = j$ is a special case: the smallest aggregate falls on the boundary between two intervals, the largest falls on the next highest boundary, and so all the aggregates fit within a single interval.

Suppose that we represent the PSD by $\{N_i\}$, the number concentrations of particles inside each interval, and that the average particle volume inside the i^{th} interval is assumed to be a constant, $\bar{v}_i$. (An appropriate choice would be the average of the two bounds of the interval.) The rate of aggregation between particles in intervals i and j is $(\beta_0\beta_{i,j}N_iN_j)$, where $(\beta_0\beta_{i,j})$ is the aggregation kernel. ($\beta_{i,j}$, with dependence on i and j, gives size-dependent aggregation, but we implicitly approximate it as constant inside intervals.) To reconstruct the method of Hounslow, the aggregates from intervals i and j must be added to intervals $(k-1)$ and k in such a way that particle number and mass are correct. This is now a simple problem with two constraints and two unknowns. The two unknowns are ΔR_k and ΔR_{k-1}, the rates of change of N_k and N_{k-1} due to these aggregations. The first constraint is that these two rates must sum to the total rate of these aggregations

$$\Delta R_k + \Delta R_{k-1} = \beta_0\beta_{i,j}N_iN_j \tag{2}$$

and the second constraint is that total particle volume is conserved

$$\Delta R_{k-1}\bar{v}_{k-1} + \Delta R_k\bar{v}_k = \beta_0\beta_{i,j}N_iN_j(\bar{v}_i + \bar{v}_j) \tag{3}$$

The solution to these equations is

$$\Delta R_{k-1} = \beta_0\beta_{i,j}N_iN_j(\bar{v}_k - \bar{v}_i - \bar{v}_j)/(\bar{v}_k - \bar{v}_{k-1}) \tag{4}$$

$$\Delta R_k = \beta_0\beta_{i,j}N_iN_j(\bar{v}_i + \bar{v}_j - \bar{v}_{k-1})/(\bar{v}_k - \bar{v}_{k-1}) \tag{5}$$

Obviously, $\Delta R_i = \Delta R_j = -(\beta_0\beta_{i,j}N_iN_j)$.

Implementation of the New Formulation

The following is a step-by-step guide to the implementation of this formulation. This calculates the total rate of change of each N_i, which we here call R_i. These rates of change will then be integrated using a solving routine for ordinary differential equations. The procedure starts by initializing all these rates to zero

$$R_i = 0 \quad \text{for all} \quad i \tag{6}$$

All (i, j) combinations must be considered, maintaining $i \le j$ to avoid double-counting. So, i is looped through all intervals ("from 1 to N", if 1 is the first interval and N is the number of intervals). For each i, then j is looped through all intervals greater than or equal to i ("from i to N").

For each (i, j) combination reached in this way, let R be the rate of aggregation between these two intervals

$$R = \begin{cases} \beta_0\beta_{ij}N_iN_j & \text{for } i \ne j \\ \frac{1}{2}\beta_0\beta_{ij}N_iN_j & \text{for } i = j \end{cases} \tag{7}$$

This rate is subtracted from the relevant intervals

$$R_i \leftarrow R_i - R \tag{8}$$

$$R_j \leftarrow R_j - R \tag{9}$$

where the arrow indicates "is replaced by" an action often commanded by the equals sign in computer languages. Both of these commands should be applied, even if $i = j$.

The next step is to make the corresponding additions to the recipient intervals, intervals $(k-1)$ and k. These are defined, and k must be found, such that Eq. 1 is satisfied. The method for this will depend on how the grid sizes are chosen; for example, if all the grid sizes are in a single geometric progression with ratio r, then there is a simple formula

$$k = \text{Ceiling}\left[1.0 + \ln\left(\frac{v_i + v_j}{v_1}\right)\Big/\ln(r)\right] \tag{10}$$

where the function "Ceiling" rounds any number with a fractional part up to the next highest integer. To avoid incorrect roundup of slight overestimates (due to finite-precision arithmetic), computer implementations of this equation should replace 1.0 by 0.99999 or similar.

The additions to intervals $(k-1)$ and k are calculated from Eqs. 4 and 5, which can be compactly implemented as follows

$$p = \frac{\bar{v}_k - \bar{v}_i - \bar{v}_j}{\bar{v}_k - \bar{v}_{k-1}} \tag{11}$$

$$R_{k-1} \leftarrow R_{k-1} + pR \tag{12}$$

$$R_k \leftarrow R_k + (1-p)R \tag{13}$$

where, for debugging purposes, it may be helpful to note that the proportion p should fall between 0 and 1. For large values

of i and j, then k and $(k - 1)$ may be "out of bounds"—that is, larger than the array size of R (which has the same size as N). This should be tested for before implementing Eq. 12 and Eq. 13; the out-of-bounds contributions can be simply ignored, or they can be added to a running total, which will indicate when too many particles are being lost (that is, when the upper bound of particle size is too low). Once Eqs. 7 to 13 have been enacted, the next (i, j) combination can be considered. Once all the combinations have been considered, each rate R_i has been calculated.

This new formulation is simpler to implement than the original, but, as presented, has no numerical advantages. However, it does introduce some new flexibility. For example, the size intervals no longer need to be in a single geometric progression, so long as all two-interval convolutions fit within two intervals. In practice, this means that extra detail can be added at small sizes; this can be useful, as shown in the example below. The only complication that this brings is in the determination of k for each (i, j) combination. So, for example, if the grid is defined as a fine geometric progression at small sizes and a coarser one at large sizes, then it is necessary to test whether $(v_i + v_j)$ falls within the fine or coarse domain; this dictates whether the fine or coarse version of Eq. 10 is required. Once k has been found—if necessary by systematically trying all possible values until Eq. 1 is satisfied—then all other steps are as above.

Variations on this Method

Now suppose that the discretized quantity representing the PSD is not N_i, but rather a point-value of the number density $n_i \approx n(v_i)$. We will shift the intervals so that mean volume $\bar{v}_i = v_i$. We will need to have a quantity a_i, such that $N_i = (a_i n_i)$ and the total volume concentration is $(a_i n_i \bar{v}_i)$. This a_i will obviously be connected to the width of the interval, but it need not be exactly the same. The choice of a_i relates to how integration is performed on functions related to the PSD, and three options are now discussed. In particular, the moments m_j of the PSD are often required. For consistency with earlier work, we will use length-based moments

$$m_j = \int_0^\infty v^{(1/3)j} n(v)\, dv \tag{14}$$

and approximate them from the number densities using coefficients $\mu_{i,j}$

$$m_j \cong \sum_{\text{all } i} \mu_{i,j} n_i \tag{15}$$

Option 1

The original method (Hounslow et al., 1988; Litster et al., 1995), using N_i's, assumed constant number density inside each interval

$$m_j \cong \sum_{\text{all } i} (\bar{v}_i)^{(1/3)j} N_i \tag{16}$$

(Strictly speaking, this corresponds to $n(v)$ being a delta-function at each $\bar{v}_i$, but the formula for a flat interval gives very similar results.) The same assumption on n_i's gives $\mu_{i,j} = a_i (v_i)^{(1/3)j}$. The interval width is used for a_i; the interval has been shifted so that it is centered on v_i, giving $a_i = 2v_i(r - 1)/(r + 1)$.

Option 2

Alternatively, all integrations can be estimated by converting to log-size, so that a geometric progression becomes a uniform spacing, $\ln(r)$. With uniform spacing, standard quadrature rules can be used

$$\int f(v) n(v)\, dv = \int f(v) n(v) v\, d(\ln v) \cong \sum f(v_i) n_i v_i \ln(r) \tag{17}$$

This implies $a_i = v_i \ln(r)$ and $\mu_{i,j} = a_i (v_i)^{(1/3)j}$.

Option 3

Third, a continuous number density distribution can be reconstructed from the point-values by linear interpolation. This is equivalent to multiplying every n_i by a triangular spike, rising linearly from zero at v_{i-1} to unity at v_i, then returning linearly to zero at v_{i+1}. This triangular spike can be integrated to give $\mu_{i,j}$. By this definition, the spike's mean particle volume is not v_i, so in the results that follow it have been shifted by an appropriate factor, $(1/3)\,(r + 1 + 1/r)$, which gives $a_i = (3/2)\, v_i (r - 1/r)/(r + 1 + 1/r)$.

These three options have quite different justifications, but they effectively differ only in their choice of the constant (a_i/v_i). Even these differences are slight: for $q = 4$, for example, the constants are 0.1729, 0.1733 and 0.1724, respectively. Nevertheless, when used in the adapted Hounslow method, they give different results.

The conversion of the previous section's method from N_i's to n_i's is trivial, and it is constantly required; the number concentration inside an interval N_i is required to calculate the rate of aggregation events, so it is deduced from the number density n_i using a_i. This rate gives changes in particle concentrations, which are then converted back to find the effect on n_i's. In other words, it is more natural to use N_i's than n_i's for aggregation; concentrations of particle volume (rather than number) would be an equally natural choice (Verkoeijen et al., 2002). The use of n_i's, however, inspires more variations, such as Option 2. For numerical integration of analytically known PSDs, this option is dramatically better than the other two. For instance, in the test-cases below, with $q = 2$, the error in the estimate of the initial m_3 is 1% with Option 1; 2% with Option 3; and less than 10^{-6}% with Option 2.

The three options were applied to two test-cases of batch aggregation: namely, the cases Ia and Ib used on the original method (Litster et al., 1995). These both start from exponential size distributions and have analytical solutions. Case Ia applies size-independent aggregation until $I_{\text{agg}} = 0.98$. (If m_0^ϕ is the initial value of m_0, then the index of aggregation I_{agg} is $1 - m_0/m_0^\phi$.) Case 1b applies the sum kernel, $\beta(u, v) = (u + v)$, until $I_{\text{agg}} = 0.95$. As in the original work, the error in the

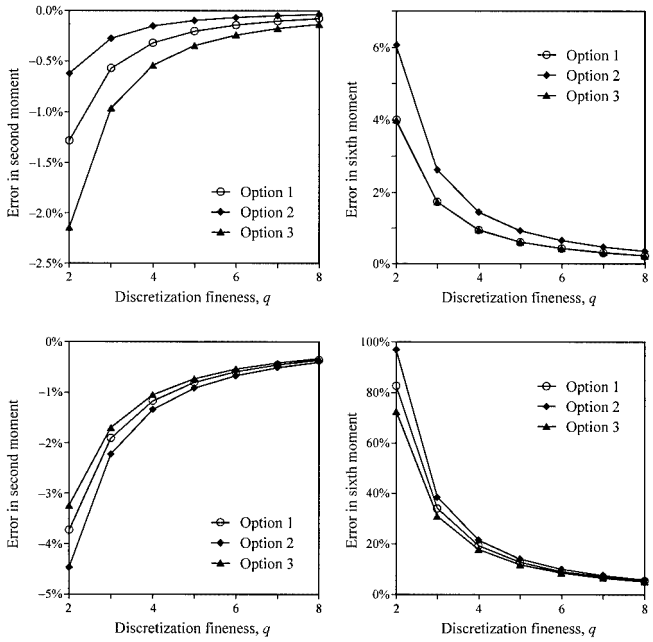

Figure 1. Errors in the moments for the two test cases.

Upper and lower rows: Cases Ia and Ib, respectively. Left and right columns: m_2 and m_6, respectively.

simulated PSDs is gauged by the errors in m_2 and m_6. The results are shown in Figure 1; the errors are defined as the percentage deviations from the analytically known results.

The errors from the three options are seen to have small but noticeable differences. (Similarly, the errors from Option 1 seem to be slightly different from the original article's, mostly smaller, even though it was intended to be a reconstruction. The trends are identical, however.) No option is obviously best in all cases. Option 3 might be discounted because it is not obviously best despite using more complicated formulas than the other two. Option 2 is marginally favored because it is a better integration scheme, as noted earlier. The value $(a_i/v_i) = \ln(r)$ is less biased than the others for the tested cases.

Option 3 does give an intuitive explanation for why m_6 is over-predicted by all the methods. The convolution of two intervals is shown in Figure 2, together with its resulting representation by two triangular spikes. The representation in the PSD is obviously broader than the correct convolution (a convolution fits *within* two intervals), and so it has an incorrectly large contribution to m_6. This is not a consequence of choosing Option 3; it is an inevitable result of the discretization approach. It might even be expected that Options 1 and 2 would suffer more from this problem than Option 3, because their convolutions are more than one interval wide, and are "stretched" to occupy two intervals; whereas in Option 3, the convolutions are more than two intervals wide and are stretched to occupy three—potentially a smaller percentage stretch. However, PSDs frequently have exponential character, which is resistant to linear approximation, and this may be why Option 3 is not the best method.

Application to Particles in Flames

The new formulation of the Hounslow DPB has been applied to the situation of silica particles in flames. Formation of small particles in flames is an industrially important process, for example, in fumed silica, titanium dioxide, and carbon black (Ulrich, 1984). When particles are significantly smaller than the mean free path of the surrounding gas, the particle-particle collisions are in the free-molecular regime. If all collisions are assumed to result in aggregation, then the aggregation kernel is given by (Friedlander, 1977)

$$\beta_0 = \left(\frac{3uM_r}{4\pi\rho}\right)^{(1/6)}\left(\frac{6k_BT}{\rho}\right)^{(1/2)} \tag{18}$$

and

$$\beta_{i,j} = (i^{-1} + j^{-1})^{(1/2)}(i^{(1/3)} + j^{(1/3)})^2 \tag{19}$$

where u is the atomic mass constant M_r is the relative molecular mass, ρ is the particle density, k_B is Boltzmann's constant, and T is the absolute temperature. Here, i and j represent the numbers of molecules in the two colliding particles.

For some systems, it has been demonstrated that effectively all collisions result in aggregation—for example, soot from a propane torch (Friedlander, 1977), carbon black, molten lead, and titanium dioxide (Ulrich, 1984). For silica, however, growth of particles has sometimes been found to be much slower than this assumption would predict; a factor of 0.004 was required to slow down the rate sufficiently to fit some experiments (Ulrich et al., 1976). The authors of that work considered this factor "unrealistically small," and proposed that coalescence may be a rate-limiting factor. Coalescence has the potential to explain why silica differs from, say, titania, because silica has an anomalously high viscosity—a factor of 10^5 higher than titania. Models for coalescence rates can be used in

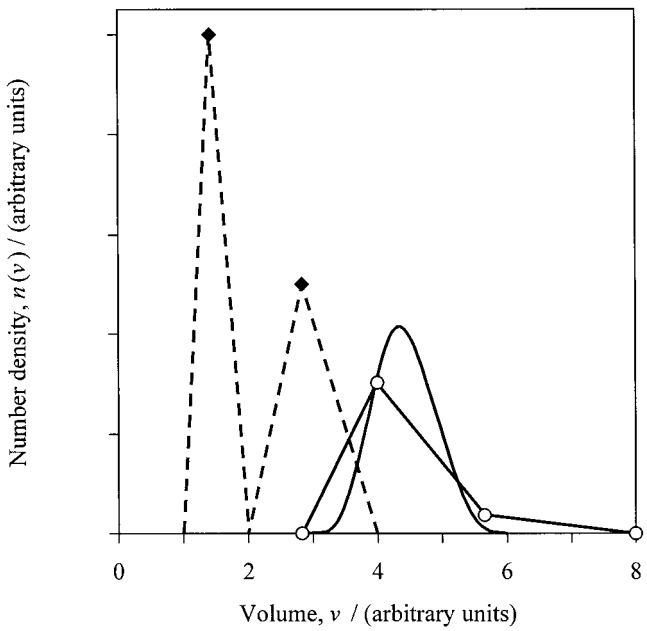

Figure 2. Illustration of errors intrinsic to discretization.

In a discretization with $q = 2$, two triangular spikes in the ranges [1, 2] and [2, 4] (broken lines) have an analytical convolution in the range [3, 6] (solid curve), but the discretized representation (solid lines) has a larger range.

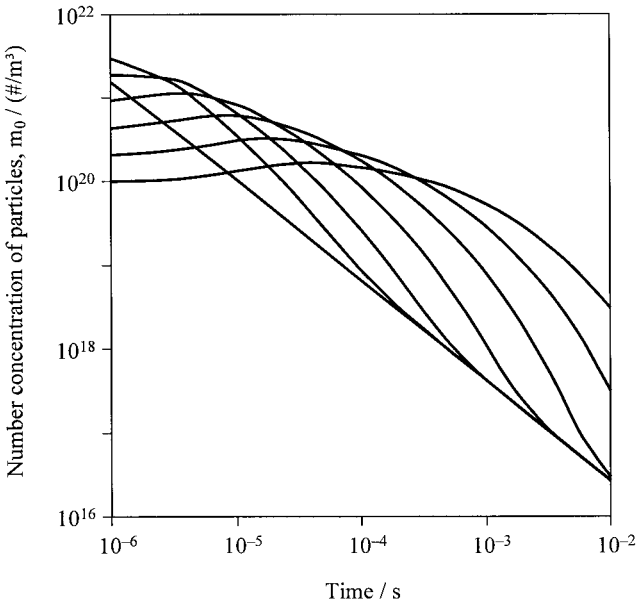

Figure 3. Variation of total particle number concentration m_0 with time for different values of the equilibrium ratio γ.

The straight line is $\gamma = 0$; to the right of it are curves for $\gamma =$ 5, 10, 20, 40, 80, and 160, respectively.

simulations (Ulrich et al., 1977). However, finite rates of coalescence cannot properly explain why silica particles grow more slowly than expected, because uncoalesced clusters have higher collision diameters and faster aggregation rates in the free-molecular regime (Wu and Friedlander, 1993). Also, the proposed rates of coalescence seem to be incompatible with some observations of large spheres of silica from short residence times in flames of moderate temperature (Zhu and Pratsinis, 1997; Ulrich, 1984; Katz et al., 1990).

An alternative effect that may slow down growth of silica particles is the chemistry of the species involved. A silicon-containing additive may decompose extremely rapidly, but the products may be SiO, SiO_2, and possibly $OSi(OH)_2$ and so on in equilibrium (Butler et al., 2002). At temperatures above the dew point of SiO, only SiO_2 will contribute to growing particles. The equilibrium

$$SiO + OH \leftrightarrows SiO_2 + H \tag{20}$$

is expected to give a constant ratio $\gamma = [SiO]/[SiO_2]$, so that there is a "pool" of SiO ready to replace SiO_2 molecules when they are involved in aggregation. This forms a source term of new molecules for aggregation. This equilibrium will apply to all silica-producing flame reactors, but its importance obviously depends on the concentrations of the OH and H radicals, which are typically defined by the fuel-oxygen composition of the flame. Other reactions have been ignored, including the fast reaction of silicon atoms

$$Si + OH \leftrightarrows SiO + H \tag{21}$$

and the participation of nonsilica molecules in particle formation.

This situation has been simulated using the new formulation of the Hounslow DPB. A discrete-sectional approach was used—in other words, the smallest particles were noted as integer numbers of molecules, but the PSD at larger particles was represented by more widely-spaced values. This follows the approach of previous discrete-sectional approaches (Wu and Flagan, 1988; Landgrebe and Pratsinis, 1990), but is much simpler to implement. The discrete region is regarded as delta-functions at the integer multiples of molecules, and, thus, automatically satisfies the constraint that convolutions should fit within two intervals. The sectional region was chosen to be a standard geometric progression.

Results are shown in Figures 3 and 4 for different values of γ, all with the same temperature, namely 2,400 K, and the same mole fraction of SiO and SiO_2 in total, namely 0.005. It can be seen in Figure 3 that, for $\gamma = 0$, the total number concentration of particles m_0 decreases effectively as a straight line on a log-log plot. For increasing values of γ, however, m_0 initially stays constant and even increases slightly. Perhaps surprisingly, m_0 then approaches the same line as $\gamma = 0$. Similarly, in Figure 4, the increase in mean particle volume (or, equivalently, the mean number of molecules per particle) is linear for $\gamma = 0$, and all curves for larger values of γ approach this. If the time taken to converge is less than the residence time (as it might be, say, for $\gamma = 10$ and a residence time of a few milliseconds), then it appears that the final PSD is not at all affected by the delayed source term represented by γ. For larger values of γ, the mean size is smaller, even when effec-

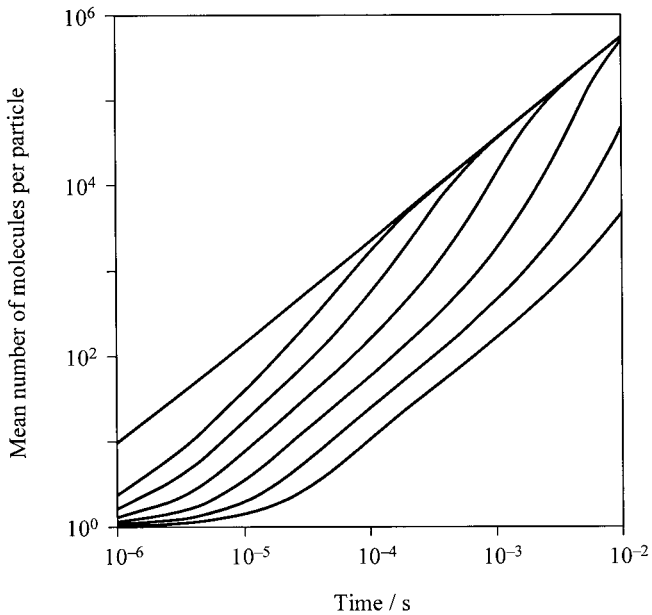

Figure 4. Variation of mean particle volume with time, for different values of the equilibrium ratio γ.

The straight line is $\gamma = 0$; to the right of it are curves for $\gamma =$ 5, 10, 20, 40, 80, and 160, respectively.

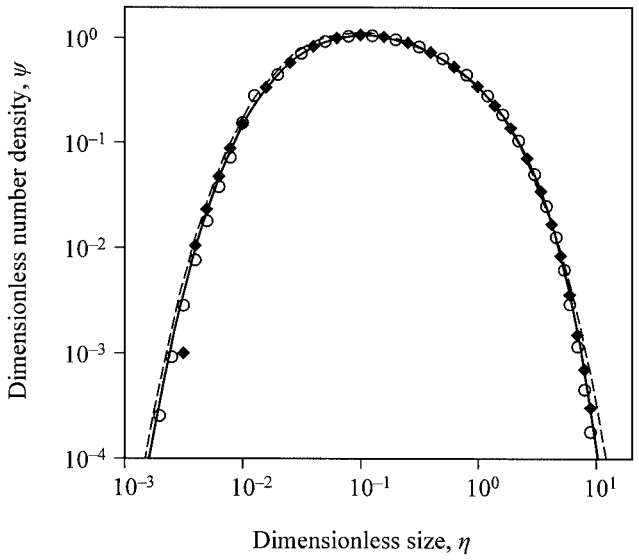

Figure 5. Comparison of calculations of the classical Self-Preserving Size Distribution ($\gamma = 0$) by various methods.

(◆—selected values from Vemury et al. (1994); ○—selected values of $\psi_{LF}(\eta)_{\text{norm}}$ from Graham and Robinson (1976); broken line—new method, using Option 2 and $q = 2$; solid line—new method, using Option 2 and $q = 16$.)

tively all the molecules have been liberated into the active form. This reduced mean size is influenced by the pool of single molecules and small clusters; faster convergence can be seen in other versions of mean size that are more weighted by larger particles, for example the $v_{6,3}$ mean rather than the $v_{3,0}$ shown in Figure 4.

The results for $\gamma = 0$ agree well with published results, as shown in Figure 5, so long as q is sufficiently high. (The results for $q = 4$ are almost indistinguishable from those shown with $q = 16$.) See the next section for a definition of the dimensionless groups. The results of Graham and Robinson (1976) are seen to be slightly different from the more accurate results of Vemury et al. (1994), although the first point of the latter is probably a misprint: at $\log_{10}(\eta) = -2.5$, ψ should be 0.0040 (or indeed 0.0039) rather than 0.0010. The implementation of the new DPB formulation is exceedingly simple. The two regions give different weighting coefficients a_i and k cannot be found for all i and j using a single formula, but, apart from that, all intervals are treated in the same way as for a single geometric progression. This shows that the formulation is simple, flexible, and accurate.

Summarized Model for Aggregation with Source of New Molecules

Without a source term, aggregation in the free-molecular regime causes the PSD to tend quickly towards a self-preserving size distribution (SPSD) (Friedlander, 1977). It is self-preserving in that it can be scaled to a dimensionless distribution ψ, which is a known function of dimensionless size only $\eta \equiv (vN/V)$

$$n(v) = N^2\psi(\eta)/V \tag{22}$$

where N is the total number concentration of particles, and V is the total volume concentration. With no source term, V is constant, but N decreases due to aggregation, at a known rate

$$\frac{dN}{dt} = -\frac{\alpha}{2}\beta_0\left(\frac{V}{v_0}\right)^{(1/6)} N^{(11/6)} \tag{23}$$

where v_0 is the volume of a single molecule and α is a numerically known constant, approximately 6.55 (Graham and Robinson, 1976). This single differential equation can be used to simulate the progress of the PSD, even if the starting-point does not closely resemble the SPSD—for example, only single molecules (Vemury et al., 1994).

The SPSD (which, henceforth, in this work refers only to the specific SPSD for free-molecular aggregation without source terms) is self-preserving, because there is only one phenomenon at work, and it has a consistent effect at different length-scales. For the system described in the example above, however, there are two distinct length-scales: the large particles, with increasing mean size, and the single molecules and small clusters. Only two parameters, N and V, are required to define the SPSD, but it is clear that more parameters will be required for systems with a source of single molecules.

However, in the results from the previous section's example, it was observed that the larger particles strongly resemble the full-participation SPSD, presumably because the tendency of these particles to approach the SPSD outweighs the disturbances from the smaller particles. The smaller particles' PSD frequently resembles the equation

$$n_i \approx n_1 i^{-b} \tag{24}$$

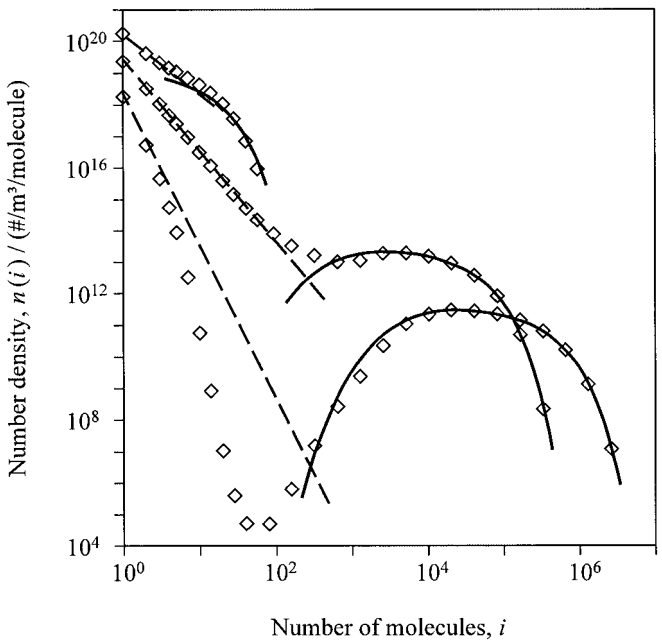

Figure 6. Particle-size distributions for $\gamma = 80$.

The PSDs are shown for three times: 0.02, 1, and 2 milliseconds. Lines are the summarized model, with broken lines for the smaller region and solid curves for the large. Open squares are from detailed simulation using the PBEs. Agreement is seen to be excellent.

This observation is demonstrated below in Figure 6. Therefore, simulated PSDs for a wide range of times can be summed up using only four parameters: N, V, n_1, and n_2. (The index b can be deduced from the number of concentrations of monomers and dimers n_1 and n_2.) It is now shown that the variation of these parameters (on the assumption that they are a valid description) can be predicted by a sequence of approximations. In a sense, this is a quasi-self-preserving size distribution, similar to those used in the transition regime (Vemury et al., 1994), in that there is no guarantee that the PSD will continue to have two regions resembling Eq. 24 and the SPSD.

One key approximation expresses the size-dependent part of the aggregation kernel as a sum of powers

$$\beta_{i,j} = \left(\frac{1}{i} + \frac{1}{j}\right)^{(1/2)} (i^{(1/3)} + j^{(1/3)})^2 \cong i^{-(1/2)} j^{(2/3)} \sum_{k=0}^{K} c_k (i/j)^{(1/3)k} \tag{25}$$

The fractional powers of (i/j) are inspired by the power-series expansion of the exact form. Suitable coefficients can be found using discrete Chebyshev polynomials (Spanier and Oldham, 1987). Using $K = 3$, with coefficients $c_0 = 0.997$, $c_1 = 2.177$, $c_2 = -0.116$, and $c_3 = 2.590$, this approximation is accurate to within $\pm 0.5\%$ whenever $i \leq j$. The advantage of this approximation is that it is amenable to analytical treatment; for example, the rate of death of monomers due to collisions with particles in the SPSD is

$$\begin{aligned} \beta_0 n_1 \frac{N v_0}{V/N} \int \beta_{1,j} \psi\left(\frac{j v_0}{V/N}\right) dj & \\ \cong \beta_0 n_1 \frac{N v_0}{V/N} \sum_{k=0}^{K} \left[c_k \int j^{(1/3)(2-k)} \psi\left(\frac{j v_0}{V/N}\right) dj \right] & \\ \cong \beta_0 n_1 N \sum_{k=0}^{K} \left[c_k J^{(1/3)(2-k)} \int \eta^{(1/3)(2-k)} \psi(\eta)\, d\eta \right] & \end{aligned} \tag{26}$$

In the last line of this equation, the integrals' limits can be regarded as 0 to ∞, so the integrals are, therefore, simply fractional volume-based moments of the dimensionless SPSD, for which numerical values have been published (Vemury et al., 1994). The mean number of molecules in the SPSD particles is J, equal to $V/(N v_0)$.

Another very useful expression approximates the sum of powers of integers (Spanier and Oldham, 1987)

$$S(v, I) \equiv \sum_{i=1}^{I} i^v \cong \zeta(-v) + \frac{I^{v+1}}{v+1} + \frac{I^v}{2} + \frac{v I^{v-1}}{12} + \cdots \tag{27}$$

where ζ is the Riemann zeta function. For example, the rate of death of monomers due to collisions with the "smaller" particles (that is, those obeying Eq. 24, including the monomers themselves) is

$$\beta_0 n_1 \sum_{i=1}^{I} \beta_{i,1} n_i \cong \beta_0 n_1^2 \sum_{k=0}^{K} \left[c_k \sum_{i=1}^{I} i^{-b+(1/3)(2-k)} \right] \tag{28}$$

Here, I marks the transition from the smaller region to the larger; it can be deduced from the PSD's four parameters. The inner sums of Eq. 28 can be approximated by the first few terms of Eq. 27.

The two terms, Eq. 26 and Eq. 28, represent the entire death rate of monomers; once the source term is added, they give the rate of change of n_1, as in Eq. A1. Similar expressions can be found for the rate of change of n_2, with a source term equal to $(1/2)\, \beta_0 \beta_{1,1} (n_1)^2$. In the SPSD-like region, the number concentration N is assumed to reduce due to internal collisions by a rate given by Eq. 23. Aggregation of a larger particle with a smaller particles does not change N, because the result is a larger particle. The rate of addition to N from smaller-smaller aggregations can be estimated in the same way as Eq. 28, choosing the limits of summation to give aggregates larger than I. Details are given in the Appendix. The rate of increase of V can be estimated in similar ways, but it is simpler and more accurate to deduce it from a mass balance.

Thus, the simulation of the PSD can be reduced from some hundreds of differential equations in the discrete-sectional approach (or many millions in a purely discrete approach) to four—or three, if V is calculated by mass balance. Results are given in Figure 6, and compared to results from the discrete-sectional method described earlier. It can be seen that the assumption of the two regions, Eq. 24 and the SPSD, is fully justified for much of the time. The main disparity is at large times, when the detailed simulation gives a curved "smaller" region rather than a straight line on the log-log plot. At this stage, these clusters of dozens of molecules are insignificant; the single molecules that arrive from the source term are quickly scavenged by the larger particles. This is therefore an acceptable error. The trends of mean size, distribution width, and yield of larger particles are followed extremely well by the quasi-self-preserving model; examples can be seen in Figure 6. This is remarkably successful, considering that the model started from monodispersity (with some small token values in n_2, N and V to avoid division-by-zero difficulties) and a nominal transition-point of $I = 2$.

The success of the model depends on the observation that detailed simulations gave PSDs with two regions as assumed. It is reasonable that the larger particles should adopt the SPSD, because arbitrary collections of particles always approach this. As yet, there is no rationale behind Eq. 24, and so this model should not be applied blindly. However, any source term of comparable rate to those used here can be expected to behave in a similar way. When the source term becomes negligible (such as when the reaction is exhausted in the present system), the power-law region quickly becomes irrelevant, and the success of the power-law approximation is unimportant; the SPSD region will be correctly followed. If the source term is very large, the small particles are dominated by single molecules, which are tracked approximately by the method. It can, therefore, be expected that the two-region assumption will be applicable in a wide range of systems. It is reassuring to note that simulations with different source terms give PSDs that strikingly resemble the two-region assumption: for example, Figure

3b of Xiong and Pratsinis (1991), where the source term is continuous oxidation of $TiCl_4$ to TiO_2.

Stiffness of Aggregation Equations

The equations in the previous section summarized the effect of the entire PSD aggregating with itself, and, thus, reduced the problem to a few equations. Another application of this is to investigate the stiffness of the detailed simulation of aggregation. Stiffness is a numerical difficulty that is encountered in solving differential equations with widely different timescales (Dekker and Verwer, 1984); this difficulty has been identified in simulations of aggregation equations, and stiff equation solvers are typically used (for example, Xiong and Pratsinis, 1991). The summarized model can be used to show that this stiffness originates from collisions between small and large particles, especially when either small or large particles form the majority.

If we consider the evolution of the SPSD without a source term, then Eq. 23 shows that the overall timescale is $[(1/2)\,\alpha\beta_0 \mathrm{J}^{1/6}\mathrm{N}]^{-1}$. On the other hand, when the main cause of death of single molecules is aggregation with larger particles, then Eq. 26 gives the timescale for changes in n_1. As a crude approximation to $\beta_{i,j}$, we may use $K = 0$, $c_0 = 1$, giving an n_1 timescale of $[0.9\beta_0 J^{2/3} N]^{-1}$. [The (2/3)-moment of the dimensionless SPSD is roughly 0.9 (Vemury et al., 1994).] When J has reached a large value, therefore, the timescale of reduction in n_1 is shorter than the overall timescale by a factor of order $J^{1/2}$, which may be very considerable. The value of n_1 is irrelevant by this stage, of course, but a simulation will still attempt to calculate it, and so the problem is stiff.

Similarly, at very early times, stiffness arises from the larger sizes being simulated. There are very few large particles at early times, so the main rate of change of n_j will be birth from aggregations involving n_1 and n_{j-1}

$$\frac{dn_j}{dt} \cong \beta_0\beta_{1,j-1}n_1n_{j-1} \cong \beta_0\beta_{1,j}n_1n_j \cong \beta_0 j^{(2/3)}n_1n_j \qquad (29)$$

The later lines in this equation are crude approximations, but they show that the timescale is roughly $[\beta_0 j^{2/3} n_1]^{-1}$, again a very considerable factor shorter than the overall timescale. Thus, if large sizes are included in the simulation, as they must be, they will introduce stiffness. This difficulty is entirely removed when, in the absence of a source term, the SPSD is tracked using Eq. 23. Similarly, the difficulty is alleviated when a source-term situation is tracked using the two-region model of the previous section, but this model includes the small-large interactions that cause the stiffness. This is why the differential equations are stiff, and why appropriate numerical methods are necessary. Perhaps inevitably, the source of the stiffness is an irrelevant part of the size distribution: the rate of collision between small and large particles is disproportionately high, especially early in the aggregation, when there are very few large particles, and late in the aggregation, when there are very few small ones.

Conclusions

A new formulation of the popular Hounslow DPB has been developed. This can reconstruct the results of the original formulation, for example, correctly predicting the total number and volume of particles, but it is much simpler to implement. The new formulation also has greater flexibility. For example, the discretization's spacing can be changed in different regions, so long as the convolution of all pairs of intervals will fit within two other intervals; in practice, this means that extra detail can be added at smaller sizes. Another new flexibility is in the coefficients used for integration; three options have been tested and compared.

The new formulation was applied to the formation of silica particles in flames. In particular, it was assumed that SiO_2, which forms stable particles at the flame temperature, is in equilibrium with SiO, which does not. As SiO_2 molecules deposit onto particles, new ones form from SiO. This source term of new molecules complicates the evolution of the particle-size distributions. The simulations revealed that the delayed release of the molecules initially resulted in smaller mean particles sizes, compared to the situation in which all molecules participated from the start. However, somewhat surprisingly, the difference disappeared as time progressed.

It was observed that the simulated particle-size distributions could be regarded as having two regions: power-law behavior at smaller sizes, and the known self-preserving size distribution at larger sizes. Four parameters were therefore needed to describe the distributions, and the rates of change of these parameters could be calculated approximately. This gave a quasi-self-preserving size distribution, a very efficient means of simulation. The results from this summarized model matched the detailed simulations remarkably well. The same approach gave information about the relative timescales of change in the smallest and largest particles; this diagnosed the source of the stiffness of these differential equations.

Notation

a_i = conversion factor (N_i/n_i), μm
b = index of power-law, Eq. 24
c = coefficient in power series, Eq. 25
i, j, k = number of molecules, or index in discretization, of particle
I = transition point between small and large regions
J = mean number of molecules in SPSD
K = highest power in power series, Eq. 25
m_j = j^{th} number-based moment of PSD, μm^j m^{-3}
M_j = j^{th} volume-based moment of PSD, μm^{3j} m^{-3}
n = number density of particles, No. m^{-3} μm^{-1}
N = number concentration of particles, No. m^{-3}
q = index defining $r = 2^{1/q}$
r = discretization ratio, v_{i+1}/v_i
R = rate of change of N, No. m^{-3} s^{-1}
S = sum of integer powers, Eq. 27
v = volume of particle, μm^3
V = volume concentration of particles, μm^3 m^{-3}

Greek letters

α = factor in SPSD growth, Eq. 23
β_o = size-independent part of aggregation kernel, m^3 s^{-1}
β = size-dependent part of aggregation kernel
γ = equilibrium ratio, [SiO]/[SiO_2]
η = dimensionless size, Eq. 22
$\mu_{i,j}$ = contribution of i^{th} interval to j^{th} moment, Eq. 15, μm^j
ζ = Riemann zeta function
ψ = dimensionless size distribution, Eq. 22

Literature Cited

Biggs, C. A., and P. A. Lant, "Modelling Activated Sludge Flocculation using Population Balances," *Powder Technol.,* **124,** 201 (2002).

Butler, C. J., A. N. Hayhurst, and E. J. W. Wynn, "The Size and Shape of Silica Particles Produced in Flames of $H_2/O_2/N_2$ with a Silicon-Containing Additive," *Proc. Comb. Inst.,* **29,** 1047 (2002).
Dekker, K., and J. G. Verwer, *Stability of Runge-Kutta Methods for Stiff Non-linear Differential Equations,* North-Holland, Oxford (1984).
Friedlander, S. K., *Smoke, Dust and Daze: Fundamentals of Aerosol Behaviour,* Wiley, New York (1977).
Graham, S. C., and A. Robinson, "A Comparison of Numerical Solutions to the Self-Preserving Size Distribution for Aerosol Coagulation in the Free-Molecule Regime," *J. Aerosol Sci.,* **7,** 261 (1976).
Hounslow, M. J., R. L. Ryall, and V. R. Marshall, "A Discretized Population Balance for Nucleation, Growth and Aggregation," *AIChE J.,* **34,** 1821 (1988).
Katz, J. L., D. Chin, S.-L. Chung, M. R. Zachariah, and H. G. Semerjian, "Silica-Particle Formation using the Counter-Flow Diffusion Flame Burner," *Combustion and Plasma Synthesis of High-Temperature Materials,* Z. A. Munir and J. B. Holt, eds., VCH Publishers, New York (1990).
Kumar, S., and D. Ramkrishna, "On the Solution of Population Balance Equations by Discretization—II. Nucleation, Growth and Aggregation of Particles," *Chem. Eng. Sci.,* **52,** 4659 (1997).
Landgrebe, J. D., and S. E. Pratsinis, "A Discrete-Sectional Model for Particulate Production by Gas-Phase Chemical Reaction and Aerosol Coagulation in the Free-Molecular Regime," *J. Colloid Interface Sci.,* **139,** 63 (1990).
Litster, J. D., D. J. Smit, and M. J. Hounslow, "Adjustable Discretized Population Balance for Growth and Aggregation," *AIChE J.,* **41,** 591 (1995).
Nicmanis, M., and M. J. Hounslow, "A Finite Element Method for the Steady State Population Balance Equation," *AIChE J.,* **44,** 2258 (1998).
Randolph, A. D., and M. A. Larson, *Theory of Particulate Processes,* 2nd ed., Academic Press, New York (1988).
Spanier, J., and K. B. Oldham, *An Atlas of Functions,* Hemisphere, London (1987).
Tsantilis, S., and S. E. Pratsinis, "Evolution of Primary and Aggregate Particle-Size Distributions by Coagulation and Sintering," *AIChE J.,* **4,** 407 (2000).
Ulrich, G. D., "Flame Synthesis of Fine Particles," *Chem. Eng. News,* **62,** 22 (1984).
Ulrich, G. D., B. A. Milnes, and N. S. Subramanian, "Particle Growth in Flames. II: Experimental Results for Silica Particles," *Combust. Sci. Technol.,* **14,** 243 (1976).
Ulrich, G. D., B. A. Milnes, and N. S. Subramanian, "Particle Growth in Flames. III: Coalescence as a Rate-Controlling Process," *Combust. Sci. Technol.,* **17,** 119 (1977).
Vemury, S., K. A. Kusters, and S. E. Pratsinis, "Time-Lag for Attainment of the Self-Preserving Particle Size Distribution by Coagulation," *J. Colloid Interface Sci.,* **165,** 53 (1994).
Verkoeijen, D., G. Pouw, G. M. H. Meesters, and B. Scarlett, "Population Balances for Particulate Processes—a Volume Approach," *Chem. Eng. Sci.,* **57,** 2287 (2002).
Wu, J. J., and R. C. Flagan, "A Discrete-Sectional Solution to the Aerosol Dynamic Equation," *J. Colloid Interface Sci.,* **123,** 339 (1988).
Wu, M. K., and S. K. Friedlander, "Enhanced Power-Law Agglomerate Growth in the Free Molecule Regime," *J. Aerosol Sci.,* **24,** 273 (1993).
Wynn, E. J. W., "Improved Accuracy and Convergence of the Discretized Population Balance of Litster et al.," *AIChE J.,* **42,** 2084 (1995).
Xiong, Y., and S. E. Pratsinis, "Gas Phase Production of Particles in Reactive Turbulent Flows," *J. Aerosol Sci.,* **22,** 637 (1991).
Zhu, W., and S. E. Pratsinis, "Synthesis of SiO_2 and SnO_2 Particles in Diffusion Flame Reactors," *AIChE J.,* **43,** 2657 (1997).

Appendix

This appendix details the rates of change of the four parameters n_1, n_2, N and V used to summarize the PSD for a system undergoing aggregation in the free-molecular regime, with a continuous source of single molecules. As a reminder, the summarized PSD is assumed to have two distinct regions: at small sizes, the PSD obeys Eq. 24, and, at larger sizes, the PSD is the same as the self-preserving size distribution (as calculated without a source of single molecules). The transition occurs at particles containing I molecules; I can be deduced from the four parameters. The PSD of the smaller region can be reconstructed from n_1 and n_2, the number concentrations of single- and two-molecule particles. The larger region is defined by its total number and volume concentrations of particles N and V.

By approximating the aggregation kernel as in Eq. 25, it was shown in Eq. 28 and Eq. 26 that

$$\frac{dn_1}{dt} \cong X_1 - \beta_0 n_1^2 \sum_{k=0}^{K} c_k S\left(-b + \frac{1}{3}(2-k), I\right) - \beta_0 n_1 N \sum_{k=0}^{K} [c_k J^{(1/3)(2-k)} M_{(1/3)(2-k)}] \quad \text{(A1)}$$

Here, X_1 is the source term of new single molecules; $S(v, I)$ is a shorthand for the sum in Eq. 27, which also indicates how it is approximated; and M_j is the j^{th} moment of the dimensionless SPSD. In contrast to the other moments used in this article, these are volume-based moments, for consistency with the published table of their values (Vemury et al., 1994). If the source of new molecules is the one explained above, with the active SiO_2 molecules in equilibrium with inactive SiO, having equilibrium constant $\gamma = [SiO_2]/[SiO]$, then the source term is

$$X_1 = \gamma\left(-\frac{dn_1}{dt}\right) \quad \text{(A2)}$$

From similar reasoning,

$$\frac{dn_2}{dt} \cong \frac{1}{2}\beta_0\beta_{1,1}n_1^2 - \beta_0 n_1 n_2 \sum_{k=0}^{K} c_k 2^{(1/3)k-(1/2)} S\left(-b + \frac{1}{3} \times (2-k), I\right) - \beta_0 n_2 N \sum_{k=0}^{K} [c_k 2^{(1/3)k-(1/2)} J^{(1/3)(2-k)} M_{(1/3)(2-k)}] \quad \text{(A3)}$$

The rate of loss of N due to internal aggregations in the SPSD is known from Eq. 23. Aggregation of larger particles with smaller particles does not change N. The rate of addition to N from smaller-smaller aggregations is the sum of all aggregation rates that result in particles greater than I. This rate can be expressed as one double sum

$$\sum_{j=1+(1/2)I}^{I} \sum_{i=I-j+1}^{j} \frac{\beta_0\beta_{i,j}n_i n_j}{1+\delta_{i,j}} \quad \text{(A4)}$$

but the Kronecker delta is needed to introduce a factor of 1/2 for (i, i) aggregations. The approximations are simpler to implement when the sum is broken into parts

$$\left(\sum_{i=1}^{(1/2)I}\sum_{j=I-i+1}^{I} + \sum_{i=(1/2)I+1}^{I-1}\sum_{j=i+1}^{I}\right)[\beta_0\beta_{i,j}n_in_j] + \sum_{i=(1/2)I+1}^{I}\tfrac{1}{2}\beta_0\beta_{i,i}n_i^2 \tag{A5}$$

In the last term in this equation, the size-dependence of the kernel is simple enough to use without power-series approximation

$$\begin{aligned}\sum_{i=(1/2)I+1}^{I}\tfrac{1}{2}\beta_0\beta_{i,i}n_i^2 &= \sum_{i=(1/2)I+1}^{I}\tfrac{1}{2}\beta_0 2^{(5/2)}i^{(1/6)}n_i^2\\ &= 2^{(3/2)}\beta_0\sum_{i=(1/2)I+1}^{I} i^{(1/6)}(n_1i^{-b})^2\\ &= 2^{(3/2)}\beta_0 n_1^2[S(-2b+\tfrac{1}{6},I) - S(-2b+\tfrac{1}{6},\tfrac{1}{2}I+1)]\end{aligned} \tag{A6}$$

In the double sums of Eq. A5, the power-series approximation (Eq. 25) is required. The inner sums can be approximated by the first few terms of Eq. 27. For example, after a rearrangement of the first double sum (which tends to have a much higher value than the second, which is often very small)

$$\begin{aligned}\sum_{i=1}^{(1/2)I}\sum_{j=I-i+1}^{I}\beta_0\beta_{i,j}n_in_j &\cong \sum_{k=0}^{K}\sum_{i=1}^{(1/2)I}\sum_{j=I-i+1}^{I}\beta_0c_ki^{(1/3)k-(1/2)}j^{(1/3)(2-k)}n_in_j\\ &\cong \beta_0n_1^2\sum_{k=0}^{K}\sum_{i=1}^{(1/2)I}\sum_{j=I-i+1}^{I}c_ki^{(1/3)k-(1/2)-b}j^{(1/3)(2-k)-b}\\ &\cong \beta_0n_1^2\sum_{k=0}^{K}\sum_{i=1}^{(1/2)I}c_ki^{(1/3)k-(1/2)-b}\sum_{j=I-i+1}^{I}j^{v}\end{aligned} \tag{A7}$$

where $v = \frac{1}{3}(2-k) - b$, then Eq. 27 is applied to the inner sum

$$\begin{aligned}\sum_{j=I-i+1}^{I}j^v &\cong \left(\zeta(-v) + \frac{I^{v+1}}{v+1} + \frac{I^v}{2} + \frac{vI^{v-1}}{12} + \cdots\right)\\ &\quad - \left(\zeta(-v) + \frac{(I-i)^{v+1}}{v+1} + \frac{(I-i)^v}{2} + \frac{v(I-i)^{v-1}}{12} + \cdots\right)\\ &\cong \frac{I^{v+1}}{v+1}\left[1-\left(1-\frac{i}{I}\right)^{v+1}\right] + \frac{I^v}{2}\left[1-\left(1-\frac{i}{I}\right)^{v}\right]\\ &\quad + \frac{vI^{v-1}}{12}\left[1-\left(1-\frac{i}{I}\right)^{v-1}\right] + \cdots \cong I^v i\left\{\left(1+\frac{v}{2I}+\frac{v(v-1)}{12I^2}\right)\right.\\ &\quad \left. - \frac{i}{I}\left(\frac{v}{2}+\frac{v(v-1)}{4I}+\frac{v(v-1)(v-2)}{24I^2}\right) + \cdots\right\}\end{aligned} \tag{A8}$$

The last line is reached by binomial expansion of the powers in the previous line, which is valid because the summed values of i are less than I. When Eq. A8 is substituted into Eq. A7, and a similar process is applied to the other double sum in Eq. A5, the result is an (admittedly lengthy) equation for the rate of change of N

$$\begin{aligned}\frac{dN}{dt} &= -\frac{\alpha}{2}\beta_0J^{(1/6)}N^2 + \beta_0n_1^2\sum_{k=0}^{K}c_kI^v\left[\left(1+\frac{v}{2I}+\frac{v(v-1)}{12I^2}\right)\right.\\ &\quad \left.\times S\left(w,\frac{1}{2}I\right) - \left(\frac{v}{2I}+\frac{v(v-1)}{4I^2}\right)S\left(w+1,\frac{1}{2}I\right)\right] + \beta_0n_1^2\sum_{k=0}^{K}c_k\\ &\quad \times\left[I^{v+1}\frac{(I-1)^w-(1/2\,I)^w}{w(v+1)} - \frac{(I-1)^{w+v+1}-(1/2\,I)^{w+v+1}}{(w+v+1)(v+1)}\right]\\ &\quad + \beta_0n_1^2 2^{(3/2)}\left[S\left(-2b+\frac{1}{6},I\right) - S\left(-2b+\frac{1}{6},\frac{1}{2}I+1\right)\right]\end{aligned} \tag{A9}$$

where $v = -b + \frac{1}{3}(2-k)$ and $w = -b + \frac{1}{2} + \frac{1}{3}k$. When I is much larger than 1 (that is, typically after the first microseconds of aggregation), many of these terms are negligible.

For the rate of change of V, larger-larger collisions have no effect, but smaller-larger collisions will transfer the smaller particles' volume into the larger region. This contribution to the rate is

$$\sum_{i=0}^{I}\int_{I}^{\infty}dv\,i\,v_0\beta_0\beta_{ij}n_in(v) \tag{A10}$$

which, after substitution of Eqs. 22, 24, and 28, becomes

$$\beta_0n_1Nv_0\sum_{k=0}^{K}c_kJ^{(1/3)(2-k)}\sum_{i=0}^{I}i^{-b+(1/3)k+(1/2)}\int_0^{\infty}d\eta\,\eta^{(1/3)(2-k)}\psi(\eta) \tag{A11}$$

which can be simplified to give

$$\beta_0n_1Nv_0\sum_{k=0}^{K}c_kJ^{(1/3)(2-k)}M_{(1/3)(2-k)}S(-b+\tfrac{1}{3}k+\tfrac{1}{2},I) \tag{A12}$$

There is also an equivalent to Eq. A5 for the contribution to V of smaller-smaller aggregations; this simply weights Eq. A5 with the aggregate volumes

$$\begin{aligned}v_0\left(\sum_{i=1}^{(1/2)I}\sum_{j=I-i+1}^{I} + \sum_{i=(1/2)I+1}^{I-1}\sum_{j=i+1}^{I}\right)[\beta_0\beta_{i,j}n_in_j(i+j)]\\ + v_0\sum_{i=(1/2)I+1}^{I}\tfrac{1}{2}\beta_0\beta_{i,i}n_i^2(i+i)\end{aligned} \tag{A13}$$

and is treated in the same way. The result is a rather daunting equation

$$\frac{dV}{dt} \cong \beta_0 n_1 N v_0 \sum_{k=0}^{K} c_k J^{(1/3)(2-k)} M_{(1/3)(2-k)} S\left(-b + \frac{k}{3} + \frac{1}{2}, I\right)$$

$$+ \beta_0 n_1^2 v_0 \sum_{k=0}^{K} c_k I^v \left[(1-v)\left(\frac{1}{2} + \frac{v}{4I} - \frac{v}{I^2}\right) S\left(w+1, \frac{1}{2} I\right) \right.$$

$$- \left(\frac{v}{2I} + \frac{v(v-1)}{4I^2}\right) S\left(w+2, \frac{1}{2} I\right) + I\left(1 + \frac{v+1}{2I} + \frac{v(v+1)}{12I^2}\right)$$

$$\left. \times S\left(w, \frac{1}{2} I\right)\right] + \beta_0 n_1^2 v_0 \sum_{k=0}^{K} c_k \left[I^{v+1} \frac{(I-1)^{w+1} - (1/2\, I)^{w+1}}{(w+1)(v+1)} \right.$$

$$+ I^{v+2} \frac{(I-1)^w - (1/2\, I)^w}{w(v+2)}$$

$$\left. - (2v+3) \frac{(I-1)^{w+v+2} - (1/2\, I)^{w+v+2}}{(w+v+2)(v+2)(v+1)} \right]$$

$$+ 2^{(5/2)} \left[S\left(-2b + \frac{7}{6}, I\right) - S\left(-2b + \frac{7}{6}, \frac{1}{2} I + 1\right) \right] \quad \text{(A14)}$$

However, it is preferable to use a mass-balance approach instead of Eq. A14, not least because this correctly predicts the final mass of product, which the integrated approximation does not. The mass-balance approach relies on a record being kept of the total number of molecules that have entered the system. The number of molecules in the smaller region is simply $S(1 - b, I)$, and the remainder must be (V/v_0).

Manuscript received Nov. 26, 2002, and revision received June 20, 2003.